

Recognition of LPI Radar Signal Intrapulse Modulation Based on CNN and Time-Frequency Denoising

Qinghua Hou*, Huibin Wu

Henan Polytechnic University, Jiaozuo, China

**Corresponding author: monfrog@163.com*

Keywords: LPI radar signal; SPWVD time-frequency analysis; K-means clustering; Convolutional Neural Network

Abstract: Aiming at the problem of low probability of intercept (LPI) radar signal recognition accuracy under low signal-to-noise ratio (SNR), a method for LPI radar signal recognition based on convolutional neural network (CNN) and time-frequency denoising is proposed. Firstly, the Smoothed Pseudo Wigner-Ville Distribution (SPWVD), which performs well under low SNR, is applied for time-frequency analysis of radar signals. Then, a frequency domain filter is designed using the K-means clustering method to reduce noise in the signal. Finally, the basic structure of the CNN network is studied, and a CNN network structure is designed and developed for the proposed LPI radar signal recognition system. Suitable hyperparameters are determined for it through parameter tuning. Time-frequency images are input into the CNN network to extract and learn deep features for radar signal recognition. Experimental results show that when the SNR is -8 dB, the overall recognition accuracy of 12 kinds of LPI radar signals reaches 91.67% using this method.

1. Introduction

The rapid and effective recognition of Low Probability of Intercept (LPI) radar signals is one of the core functionalities required in electronic warfare systems such as electronic support, electronic intelligence, electronic protection, and electronic attack. In practical applications, automatic radar signal recognition technology is a vital survival technique for threat identification by intercept receivers and radar emitter recognition^[1]. Conversely, radar signals should be designed with LPI characteristics^[2] to evade detection and recognition by intercept receivers. Therefore, intercept receivers must possess automatic LPI radar signal recognition capabilities, with highly reliable detection, classification, and identification abilities to preemptively recognize the presence of LPI radar signals.

During the process of identifying radar signals, feature extraction is crucial, and researchers have proposed various methods for feature extraction when dealing with different signals. For example, references^[3-4] extract features based on time-frequency analysis, while references^[5-6] extract features based on autocorrelation functions. Since time-frequency analysis methods can effectively establish the time-frequency correspondence of non-stationary signals, this method has become an effective tool for studying non-stationary signals in non-ideal environments^[7], such as Short-Time Fourier Transform (STFT)^[8], wavelet transform, and Choi-Williams distribution (CWD)^[9].

In recent years, these time-frequency analysis methods have been combined with deep learning methods and applied to LPI radar signal recognition, achieving good recognition performance. Reference^[10] designed an automatic classification recognition system combining Choi-Williams distribution and deep convolutional neural networks, with an overall recognition rate of 96.2% at a signal-to-noise ratio (SNR) of -2 dB. Reference^[11] utilized the Fourier synchrosqueezing transform and convolutional neural networks to achieve good recognition of multi-phase radar signals under low SNR. Reference^[12] combined ENN neural network classification recognition and proposed a radar signal feature extraction method based on CWD time-frequency transformation and image processing to achieve recognition of LPI radar signals under low SNR. Reference^[13] introduced sample averaging techniques and convolutional neural networks (CNN) for radar signal recognition. With a SNR of -6 dB, the overall recognition rate of 12 radar signals including BPSK, LFM, Costas, Frank, P1-P4, T1-T4 reached 93.58%. Reference^[14] used time-frequency images and CNN for radar signal recognition, analyzing the statistical characteristics of two-dimensional time-frequency images and proposing a simple dimensionality reduction and denoising method. Simulation results demonstrate that this method exhibits good recognition rates and strong generalization capabilities under low SNR conditions.

This article implements a convolutional neural network recognition method based on time-frequency features. To improve the recognition performance in noisy environments, a spectral calculation method based on SPWVD and K-means is proposed. In this method, the SPWVD spectrum of each LPI radar signal is first calculated. Then, the K-means clustering method is combined with SPWVD to design a frequency domain filter to reduce signal noise and calculate a new spectrum. Finally, the basic structure of CNN^[15] is studied, and a suitable CNN structure is designed and developed for the proposed LPI radar signal recognition system. Suitable hyperparameters are determined through parameter tuning, proposing a CNN network suitable for the aforementioned denoising method. This CNN is used to achieve automatic recognition based on novel time-frequency images.

In the experiments, 12 types of pulse compression signals defined in reference are considered as LPI signals, including all 5 types of polyphase codes and 4 types of polytime codes. Furthermore, the performance of the LPI radar signal recognition system proposed in this article is compared with those in references, considering the signal parameters and simulation conditions used in those studies. Experimental results show that this method achieves high radar signal recognition accuracy at low SNR. This research is of significant importance for addressing the challenges and issues in radar signal recognition with low intercept probability, providing valuable references for related research and applications.

2. System Model

In this section, the system structure for the proposed LPI radar signal recognition and the definition of the 12 types of LPI radar signals considered in this paper are introduced.

2.1. System Structure.

As shown in Figure 1, the classification system mainly consists of three parts: signal preprocessing, feature extraction, and classifier. In the signal preprocessing stage, the received LPI radar signal is first processed through SPWVD to obtain its time-frequency image, which can reflect the signal's instantaneous frequency and has good noise resistance. For modulation recognition of radar signals, in order to reduce the impact of noise on feature extraction, K-means clustering is used to set less frequent frequency values in the signal's time-frequency image to zero to reduce noise interference. Subsequently, a CNN is designed for feature extraction. Finally, two fully connected layers with a

specific number of neurons are used as the classifier for signal recognition.

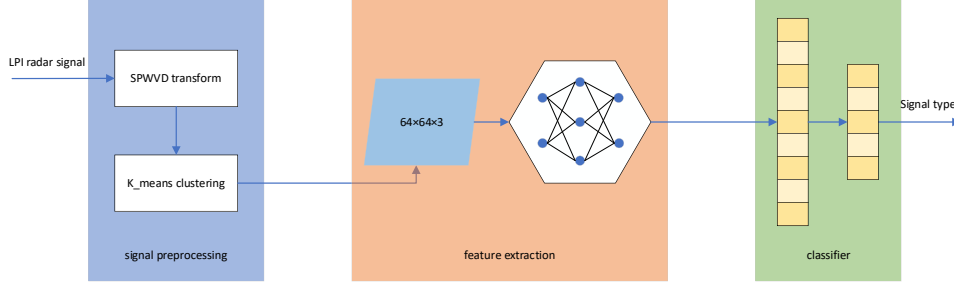


Figure 1: LPI radar signal recognition system structure

2.2. Signal Model

If the received LPI radar signal is assumed to be a pulse wave with additive Gaussian white noise, the signal model can be represented as follows

$$y[k] = x[k] + w[k] = a[k]e^{j\theta[k]} + w[k] \quad (1)$$

Where k is the sample index increment at each T_s under the sampling frequency f_s , $a[k]$ is the ideal sampled signal of the instantaneous envelope, T is the pulse duration, T_s is the sampling interval, $w[k]$ is Gaussian white noise, and $\theta[k]$ is the instantaneous phase of the ideal sampled signal. The instantaneous phase $\theta[k]$ can be defined by the instantaneous frequency $f[k]$ and phase offset $\varphi[k]$:

$$\theta[k] = 2\pi f[k](kT_s) + \varphi[k] \quad (2)$$

The difference in $\theta[k]$ determines the modulation type of the radar signal.

Table 1: 12 kinds of LPI radar signal pulse modulation functions

Signal type	$f[k][\text{Hz}]$	$\varphi_{i,j}[k][\text{rad}]$
LFM	$f_0 + \frac{B}{\tau_{pw}}(kT_s)$	fixed constant
Costas	f_j	fixed constant
BPSK	fixed constant	0 or π
Frank	fixed constant	$\frac{2\pi}{M}(i-1)(j-1)$
P1	fixed constant	$-\frac{\pi}{M}[(M-(2j-1))][(j-1)M+(i-1)]$
P2	fixed constant	$-\frac{\pi}{2M}[2i-1-M][2j-1-M]$
P3	fixed constant	$\frac{\pi}{\rho}(i-1)^2$
P4	fixed constant	$\frac{\pi}{\rho}(i-1)^2 - \pi(i-1)$
T1	fixed constant	$\text{mod} \left\{ \frac{2\pi}{N_{ps}} \left[(N_g(kT_s) - j\tau_{pw}) \frac{jN_{ps}}{\tau_{pw}} \right], 2\pi \right\}$
T2	fixed constant	$\text{mod} \left\{ \frac{2\pi}{N_{ps}} \left[(N_g(kT_s) - j\tau_{pw}) \left(\frac{2j - N_g + 1}{\tau_{pw}} \right) \frac{N_{ps}}{2} \right], 2\pi \right\}$
T3	fixed constant	$\text{mod} \left\{ \frac{2\pi}{N_{ps}} \left[\frac{N_{ps}B(kT_s)^2}{2\tau_{pw}} \right], 2\pi \right\}$
T4	fixed constant	$\text{mod} \left\{ \frac{2\pi}{N_{ps}} \left[\frac{N_{ps}B(kT_s)^2}{2\tau_{pw}} - \frac{N_{ps}B(kT_s)}{2} \right], 2\pi \right\}$

mod: The remainder obtained by dividing a by b.
[a]: The largest integer that is less than or equal to a.

The 12 kinds of LPI radar signals considered in this paper are classified into frequency modulation and phase modulation. In frequency modulation, the instantaneous frequency $f[k]$ varies while the phase offset $\varphi[k]$ remains constant. In phase modulation, $f[k]$ remains constant while $\varphi[k]$ varies accordingly. The definitions are provided in Table 1, where "Subcode" indicates partial pulse intervals, and $\varphi[k]$ is fixed as a constant within that interval. In this section, 12 types of LPI radar signals are defined as shown in Table 1, including Linear Frequency Modulation (LFM), Costas, Binary Phase Shift Keying (BPSK), 5 types of polyphase codes (such as Frank, P1, P2, P3, and P4 codes), and 4 types of polytime codes (such as T1, T2, T3, and T4 codes).

3. Signal Preprocessing

Signal preprocessing is a crucial step in the field of signal processing, as it involves operations such as noise reduction, filtering, interference removal, etc., to enhance the quality and reliability of signals. Reference proposes a spectrum calculation method for signal feature analysis using Short-Time Fourier Transform (STFT) and K-means algorithm. In this paper, a signal preprocessing method based on Smoothed Pseudo Wigner-Ville Distribution (SPWVD) and K-means algorithm is designed specifically for LPI radar signals.

Firstly, the SPWVD is utilized to perform time-frequency analysis on the signal, extracting the instantaneous frequency information of the signal and obtaining the time-frequency representation of the signal. The SPWVD transformation result for the signal $y(t)$ is as follows:

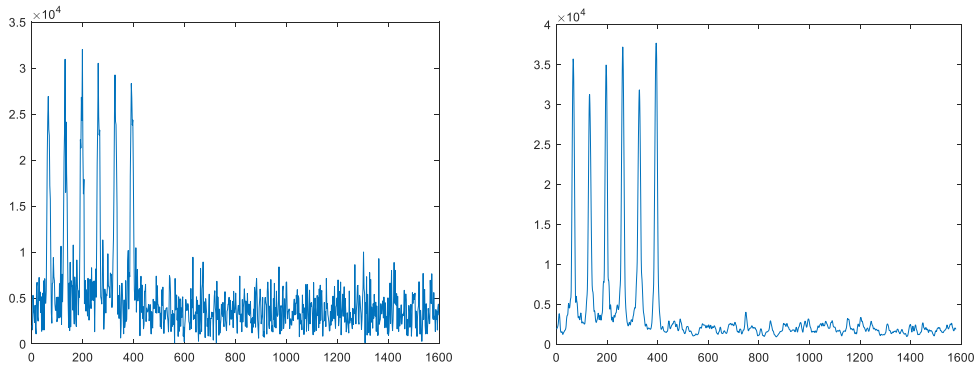
$$S(t, \nu) = \int_{-\infty}^{+\infty} h(\tau) \int_{-\infty}^{+\infty} g(s-t) y\left(s + \frac{\tau}{2}\right) y^*\left(s - \frac{\tau}{2}\right) ds e^{-j2\pi\nu\tau} d\tau \quad (3)$$

Where $h(t)$ is the window function, and $g(t)$ is the smoothing function. From the above, the SPWVD transformation of the discrete LPI radar signal $y(n)$ obtained by sampling is denoted as $S(n, k)$, where $S(n, k)$ represents the frequency change of the signal $y(n)$ along the time n . The spectrogram of the SPWVD can be represented as...

$$Sabs(n, k) = |S(n, k)| \quad (4)$$

To remove noise from the signal, in Reference a frequency domain filter is designed to eliminate redundant frequency components and noise in the spectrogram. By summing $Sabs(n, k)$ along the k -axis, i.e., adding the components on the time axis n , the frequency distribution of $y(n)$ can be obtained. This frequency classification is similar to the FT transformation of $y(n)$.

$$F(k) = \sum_{n=0}^{N-1} Sabs(n, k) \quad (5)$$



(a) FT results

(b) SPWVD results

Figure 2: Spectrum image of Costas signal

Figure 2 shows the spectrogram of a Costas signal obtained through Fourier Transform and SPWVD, with Gaussian white noise at a SNR of -2dB. It can be observed from Figure 2 that the sensitivity of SPWVD to noise is lower than that of FFT. The frequency distribution curve in Figure 2 (b) is smoother and exhibits better continuity.

Using K-means clustering to classify the elements of sequence $F(k)$ in equation (5) into different clusters, then resetting the values in the cluster with the highest mean to the centroid value, and resetting the values in the cluster with the lowest mean (considered as noise points) to zero, as shown in Figure 3.

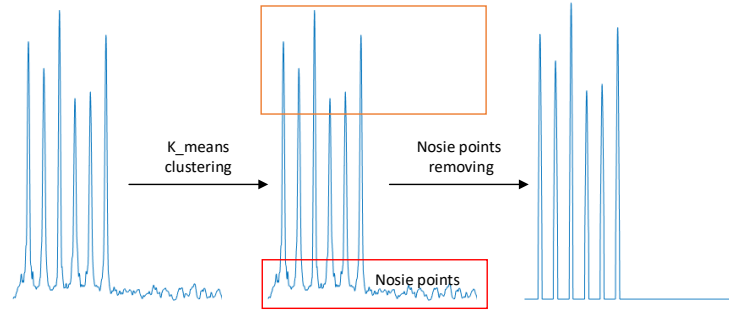


Figure 3: Noise data removal

The accurate clustering of signal noise points during the computation of the frequency domain filter directly affects the effectiveness of noise removal. Therefore, the number of clusters in the K-means algorithm becomes a key parameter. Figure 4 shows the results of processing the spectrum in Figure 2 (b) with different numbers of clusters. It can be observed from Figure 4 that the proposed method performs best when the number of clusters is 3. When the number of clusters exceeds 3, the smoothing performance decreases. Moreover, an increase in the number of clusters will increase the algorithm's complexity. Hence, the optimal number of clusters is 3, consistent with the research results in Reference.

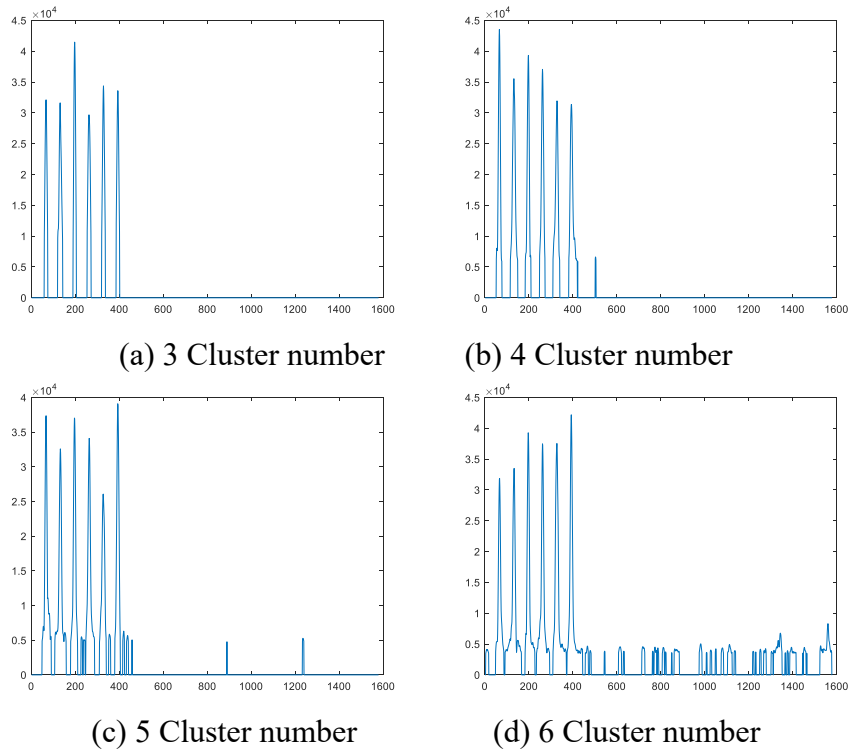


Figure 4: Spectrum images after different clustering groups

Assuming $F_a(k)$ is the generated frequency domain filter, the denoised time-frequency image is obtained:

$$S^f(n, k) = Sabs(n, k) * F_a(k) \quad (6)$$

Where $S^f(n, k)$ represents the result of signal preprocessing.

Figure 5(a) shows the new time-frequency spectrum of the Coatas signal from Figure 2, while Figures 5(b)-(d) depict time-frequency images of other types. It can be observed from Figure 5 that this method can effectively eliminate noise under low SNR conditions.

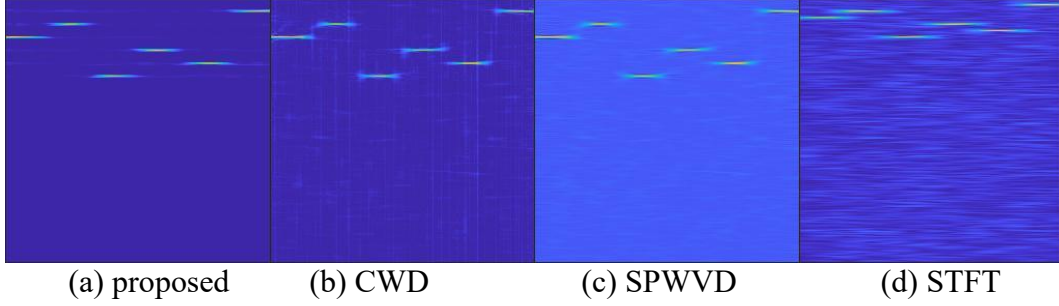


Figure 5: -2dB SNR time-frequency image of Costas signal different simultaneous frequency analysis method

4. Design of CNN

Taking into account the number of classes to be classified and the subtle shapes of the image objects of the 12 LPI radar signals, it can be seen that the problem of handwritten recognition shares many similarities with the problem considered in this paper. Therefore, based on the study of CNN in Reference an appropriate CNN is developed for the proposed LPI radar signal recognition system. The basic structure of CNN can be described using a series of functions: Input - Conv - ReLU - Pooling - Conv - ReLU - Pooling - FC - Dropout - FC, where Conv stands for the convolutional layer, ReLU represents the non-linear activation function, Pooling denotes the pooling layer, FC indicates the fully connected layer, and Dropout is the stochastic dropout layer. Building upon this basic structure, hyperparameters are designed, such as input size, number of convolutional kernels, size of convolutional kernels, and number of neurons in the fully connected layer.

By testing the recognition accuracy of 12 types of LPI radar signals at low SNR (-10dB to -6dB), adjustments are made to the input sizes of the CNN (such as 32×32 , 64×64 , and 128×128) and the number of convolutional kernels used in the first/second convolutional layers (such as 10/20, 20/40, 30/60, and 40/80). The input size is related to the resolution of objects in the images, while the number of convolutional kernels aims to identify basic visual features. Subsequently, these visual features are combined by subsequent layers to detect higher-order features.

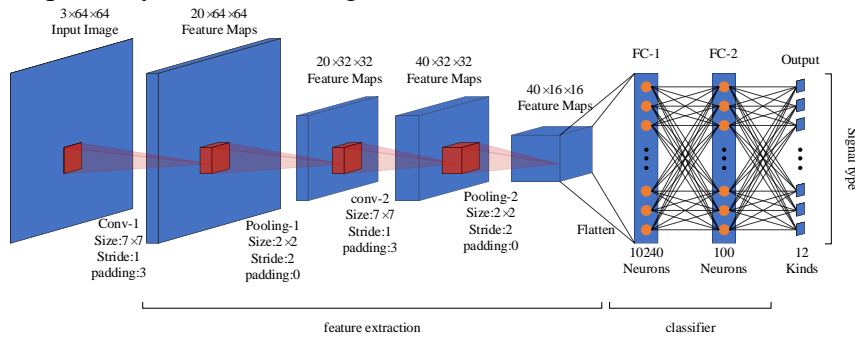


Figure 6: CNN network structure

Table 2 presents some simulation results to validate the proposed CNN design. As shown in the figure 6, an input size of 64×64 and 20 and 40 convolutional kernels for the first and second layers, respectively, yield the best performance. In the subsequent 10 rows of Table 2 (from the 13th row to the 22nd row), test results for various convolutional kernel sizes in the first and second layers are provided, assuming that the size of the first layer's kernels is greater than or equal to that of the second layer. The results indicate that, for these two layers, 7×7 kernels produce the best results. Regarding the stride size in the convolutional layers, a unit stride size is chosen as CNN needs to extract features from the subtle shapes of image objects. To determine hyperparameters in the pooling layer, max-pooling with a filter size of 2×2 and a stride of 2, without zero-padding, is employed. In the non-linear layers (omitted in Figure 6), ReLU is used as the activation function. From the last 7 rows of Table 2, it can be observed that the LPI radar signal recognition system performs best when there are 100 neurons in FC-2. For simplicity, the Dropout layers between FC-1 and FC-2 are omitted in Figure 6 to avoid potential overfitting issues. The final design details of the CNN are illustrated in Figure 6.

Table 2: Determination of CNN network hyperparameters

Input size	Conv-1 channel	Conv-2 channel	Conv-1 kernel_size	Conv-2 kernel_size	Number of neurons	accuracy/%
32×32	10	20	5×5	5×5	400	94.16
32×32	20	40	5×5	5×5	400	94.9
32×32	30	60	5×5	5×5	400	95.19
32×32	40	80	5×5	5×5	400	95.12
64×64	10	20	5×5	5×5	400	95.38
64×64	20	40	5×5	5×5	400	95.58
64×64	30	60	5×5	5×5	400	95.27
64×64	40	80	5×5	5×5	400	94.36
128×128	10	20	5×5	5×5	400	94.89
128×128	20	40	5×5	5×5	400	93.52
128×128	30	60	5×5	5×5	400	94.21
128×128	40	80	5×5	5×5	400	94.26
64×64	20	40	3×3	3×3	400	94.69
			5×5	3×3	400	94.76
			5×5	5×5	400	95.58
			7×7	3×3	400	95.08
			7×7	5×5	400	95.13
			7×7	7×7	400	96
			9×9	3×3	400	95.19
			9×9	5×5	400	95.9
			9×9	7×7	400	95.71
64×64	20	40	7×7	7×7	50	95.78
					100	96.12
					200	95.34
					300	95.16
					400	96
					500	95.69
					600	95.07

During the process of determining the hyperparameters of the network model described above, a simulated LPI radar signal time-frequency image is used as the dataset, which is divided into training, validation, and test sets. The Cross Entropy Loss function is chosen as the loss function, which is suitable for multi-classification problems and effectively measures the gap between the model's predicted results and the actual results. The optimizer selected is Adam, which combines the

advantages of Adagrad and RMSprop, allowing for adaptive adjustment of the learning rate and accelerating the convergence speed of the model. The learning rate, batch size, and epochs are set to 0.001, 64, and 35, respectively. The learning rate is reduced by half every ten epochs.

5. Simulation Experiment

This section verifies the performance of the proposed recognition system and the feasibility of the signal denoising method through simulation experiments. The section consists of three parts. The first part provides the simulation parameters for the low probability of intercept radar signals. The second part validates the effectiveness and recognition accuracy of the proposed recognition system. The third part compares the recognition accuracy of the recognition system with other systems reported in the literature.

5.1. Radar signal data generation

In the experiment, 12 simulated LPI radar signals were generated for training, validation, and testing purposes. To make the simulated signals similar to real signals, the parameter values of the signals were randomly set within specified ranges, and Gaussian white noise with different SNR was added to the signals. The parameters of each signal are shown in Table 3. The signal sampling rate is $f_s = 50\text{MHz}$. Each signal generates 600 data points, and the SNR varies from -10 dB to 6 dB in 2 dB increments. After generating these signals, the proposed SPWVD-K_means method is used to transform the signals into time-frequency images. The dataset is divided into three parts, with a data ratio of 4:1:1 for the test set, validation set, and training set, respectively.

Table 3: Setting of 12 LPI radar signal parameters

signal	simulation parameter	parameter scale
LFM	carrier frequency f_0	$[f_s/8, f_s/4]$
	bandwidth B	$[f_s/12, f_s/8]$
Costas	fundamental frequency f_{min}	$[f_s/50, f_s/40]$
	Frequency hop h	$[6, 10]$
BPSK	carrier frequency f_0	$[f_s/8, f_s/4]$
	Barker code length L_c	$\{7, 11, 13\}$
	Phase code period C_{pp}	$[6, 10]$
Frank, P1, P2	carrier frequency f_0	$[f_s/8, f_s/4]$
	Frequency step M	$[6, 10]$
	Phase code period C_{pp}	$[2, 5]$
P3, P4	carrier frequency f_0	$[f_s/8, f_s/4]$
	Subcode number N_c	$\{36, 49, 64, 81, 100\}$
	Phase code period C_{pp}	$[2, 5]$
T1, T2	carrier frequency f_0	$[f_s/8, f_s/4]$
	number of segments m	$[4, 6]$
T3, T4	carrier frequency f_0	$[f_s/8, f_s/4]$
	bandwidth B	$[f_s/12, f_s/8]$

5.2. Verify the effectiveness of the proposed system

To demonstrate the effectiveness of the proposed recognition system model in extracting time-frequency image features, 100 time-frequency images were selected as the test set for each signal at

each SNR. The confusion matrix for correctly identifying the 12 types of signals is shown in Figure 7. From the figure, it can be observed that except for signals P1 and P4, the recognition accuracy for other radar signals exceeds 94%.

Figure 8 presents the confusion matrix for the 12 types of signals at a SNR of -8 dB. Signal P1 was misidentified as P4 26% of the time, while signal P4 was misidentified as P1 24% of the time. This is mainly due to the high similarity in the time-frequency images of P1 and P4, making these two signals easily confused. Additionally, at low SNR, the presence of significant noise results in the temporal and frequency information being submerged, posing challenges to the recognition process and reducing the recognition accuracy.

From the above analysis, it is evident that each signal achieves a high recognition rate at low SNR, which effectively demonstrates the validity of feature extraction in the proposed SPWVD-K_means-CNN recognition system.

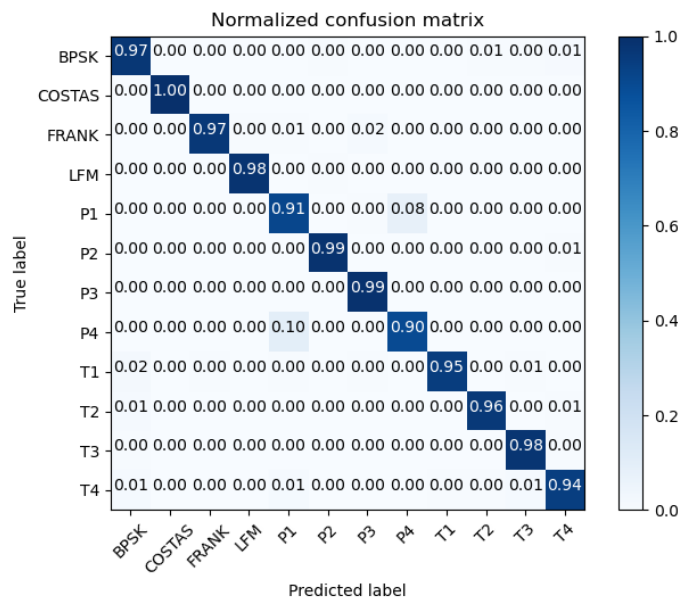


Figure 7: Identification confusion matrix of total signal

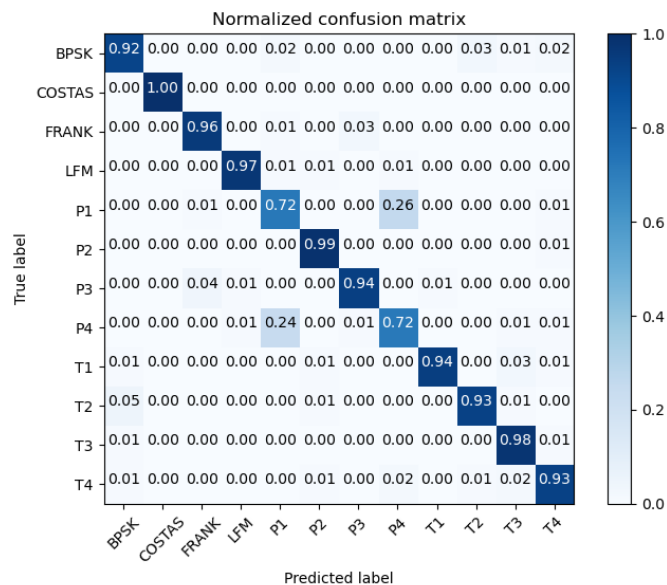


Figure 8: -8dB identification confusion matrix of 12 LPI radar signals

5.3. Performance comparison

To validate the feasibility of the proposed denoising method, experimental evaluations were conducted. The previously generated dataset and the proposed neural network were utilized to experiment with the SPWVD+K_means denoising method. In the experiment, STFT+K_means was used as a comparison experiment with SPWVD to better evaluate the effectiveness of the proposed denoising method. For the comparative experiment, the same data was processed to obtain the corresponding dataset. To assess the recognition performance of this method, it was compared with CWD-ResNet-SVM, FSST-CNN, and CWD-CNN.

Figure 9 presents the overall recognition results of the six methods at different SNR. As shown in Figure 9, when the SNR is greater than -4 dB, all methods except for CWD-ResNet-SVM exhibit high recognition accuracy, achieving over 95% recognition accuracy. As the SNR decreases, the recognition curve significantly declines. The proposed method demonstrates good recognition performance at low SNR. At a SNR of -8 dB, the recognition accuracy of this method is 91.67%, which is 4.42% higher than the best result of the other five methods. Even at a SNR of -10 dB, this method can still achieve a recognition accuracy of 78.33%, which is 3.23% higher than FSST-CNN. These results indicate that the method exhibits high recognition accuracy and strong noise resistance. Furthermore, the proposed denoising method shows better denoising effects compared to signal processing methods using STFT+K_means or SPWVD. Specifically, data processed with the proposed denoising method shows a significant improvement in SNR. This suggests that the proposed denoising method is highly feasible and practical, with the potential for wide application in real-world scenarios.

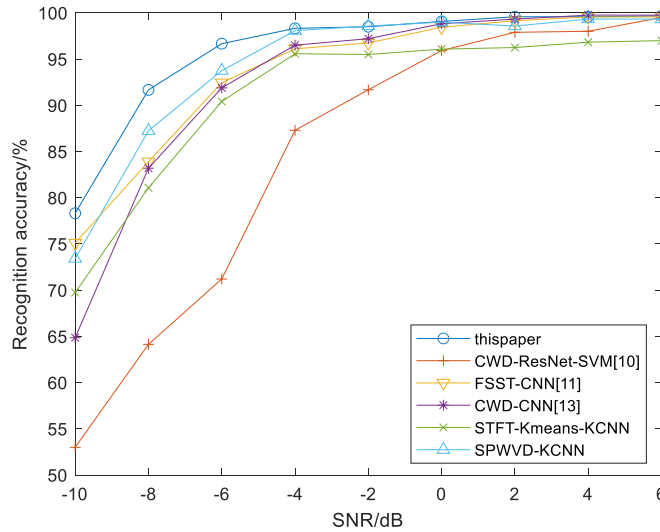


Figure 9: Performance comparison of the six methods under different SNR

6. Conclusions

This paper proposes a convolutional neural network-based method for the recognition of LPI radar signals. Firstly, a frequency domain filter is designed based on SPWVD time-frequency analysis and K_means clustering to denoise the LPI radar signals, obtaining denoised time-frequency images. Subsequently, the basic structure of CNN is studied, and a suitable CNN network structure is designed and developed for the proposed LPI radar signal recognition system, with appropriate hyperparameters determined through parameter optimization. The obtained time-frequency images are input into the CNN network to extract and learn deep features for radar signal recognition.

Experimental results demonstrate that, at a SNR of -8 dB, the overall recognition accuracy of this method for 12 types of LPI radar signals reaches 91.67%. This effectively addresses the challenges and issues in automatic identification of low probability of intercept radar signals. Compared with other methods, the proposed method exhibits higher radar signal recognition accuracy in low SNR environments and can be widely applied in fields such as electronic surveillance for the identification of real-world radar signals.

References

- [1] R. G. Wiley, *ELINT: The Interception and Analysis of Radar Signals*. Norwood, MA, USA: Artech House, 2006.
- [2] P. E. Pace, *Detecting and Classifying Low Probability of Intercept Radar*. Norwood, MA, USA: Artech House, 2009
- [3] Wang X Z. *Electronic radar signal recognition based on wavelet transform and convolution neural network* [J]. *Alexandria Engineering Journal*, 2022, 61(5): 3559-3569.
- [4] S. G. Bhatti and A. I. Bhatti. *Radar Signals Intrapulse Modulation Recognition Using Phase-Based STFT and BiLSTM* [J]. *IEEE Access*, 2022, 10: 80184-80194.
- [5] Wang C, Gao H and Zhang X D. *Radar Signal Classification Based on Auto-correlation Function and Directed Graphical Model* [C]. *6th International Conference on Signal Processing, Communications and Computing (ICSPCC)*, Hong Kong, August 2016.
- [6] Huang Z, Ma Z Y and Huang G M. *Radar Waveform Recognition Based on Multiple Autocorrelation Images* [J]. *IEEE Access*, 2019, 7: 98653-98668.
- [7] Xiao Z and Yan Z. *Radar Emitter Identification Based on Novel Time-Frequency Spectrum and Convolutional Neural Network* [J]. *IEEE Communications Letters*, 2021, 25(8): 2634-2638.
- [8] Zhang M, Diao M, Gao L, Liu L. *Neural Networks for Radar Waveform Recognition* [J]. *Symmetry*, 2017, 9(5):75.
- [9] Guo Q, Yu X, Ruan G Q. *LPI Radar Waveform Recognition Based on Deep Convolutional Neural Network Transfer Learning* [J]. *Symmetry*, 2019, 11(4):540.
- [10] Kong G Y, Koivunen V. *Radar Waveform Recognition Using Fourier-Based Synchrosqueezing Transform and CNN* [C]. *2019 IEEE 8th International Workshop on Computational Advances in Multi-Sensor Adaptive Processing*. Le Gosier, Guadeloupe: IEEE Press, 2019: 664-668.
- [11] Zhang M, Liu L T, Diao M. *LPI Radar Waveform Recognition Based on Time-Frequency Distribution* [J]. *Sensors*. 2016; 16(10): 1682-1706.
- [12] Kong S H. *Automatic LPI Radar Wave form Recognition Using CNN*. *IEEE Access*. 2018, 6: 4207–4219
- [13] Wang C, Wang J, Zhang X D. *Automatic Radar Waveform Recognition Based on Time-Frequency Analysis and Convolutional Neural Network* [C]. In *Proceedings of the IEEE International Conference on Acoustics, Speech, and Signal Processing (ICASSP)*, New Orleans, LA, USA, 2017, 2437–2441.
- [14] LeCun Y, Bottou L, Bengio Y, Haffner P. *Gradient-based learning applied to document recognition* [J], *Proceedings of the IEEE*, 1998, 86(11): 2278-2324.
- [15] Lopac N, Hrzić F, Vuksanović I P and Lerga J. *Detection of Non-Stationary GW Signals in High Noise From Cohen's Class of Time-Frequency Representations Using Deep Learning* [J]. *IEEE Access*, 2022, 10: 2408-2428.